Chapter

Study of Composite Structures Based on a Porous Silicon Matrix and Nanoparticles Ag/Zno Used as Non-Invasive Highly Sensitive Biosensor Devices

Veniamin Koshevoi, Anton Belorus, Ilya Pleshanov, Anton Timchenko, Roman Denisenko, Daniyar Sherimov and Ekaterina Vodkailo

Abstract

In this work composite structures based on a porous silicon were obtained and studied. Porous matrices were formed by electrochemical etching in aqueous solutions of hydrofluoric acid. Based on the obtained substrates, por-silicon (Si)/silver (Ag) and por-Si/zinc oxide (ZnO) composite structures were formed. These composites were functionalized by various methods (electro (E)-, thermo (T)-, electrothermal exposure) as a result of which the structures were modified. When studying the samples by scanning electron microscopy (SEM), it was concluded that silver nanoparticles actively diffused into the pores under these technological modes of functionalization. The por-Si/Ag and por-Si/ZnO composite structures were also studied using the following methods: infrared (IR) spectroscopy and Raman ultrasoft X-ray emission spectroscopy. Also, the photoluminescent characteristics of the samples were studied. Based on the obtained results, it was concluded that functionalization methods actively change the phase composition of structures and the optical properties of composites.

Keywords: porous silicon, composite structures, functionalization, nanoparticles, diffusion, phase composition

1. Introduction

One of the promising areas of science is biomedicine, which currently needs new materials and structures with certain requirements: biocompatibility, biodegradability, low toxicity, and the ability to use various methods of functionalization (post-processing) for a wide range of biologically active materials. One of the approaches to the formation of new structures is the creation of porous biocompatible matrices with deposited active particles. Due to their multifunctionality, these multilevel composite structures can be actively used as biosensors of a wide range of analytes, devices for targeted delivery of drugs, etc. [1–6].

The formation of various types of biosensors depends on the choice of material, the morphology of the sensitive layer, as well as its structural and physic-chemical properties. Various materials, such as Zn, Au, Ag, Pd, Pt, etc., as well as their modifications and composites can be used as an active layer. As an example, we can specify sensors based on various types of nanoparticles and composite structures: biosensors with zinc oxide (ZnO) nanoparticles, gold nanoparticles (AuNPs), Ag/TiO_2 nanoparticles, carbon nanotube-based biosensors, graphene quantum dot (GQD) biosensors, sensor based on the Pd/WO_3-ZnO composite porous thin films, etc. [6–17]. **Table 1** shows the sensitivity data of various composite sensor structures during glucose detection.

As already mentioned, changing the morphology and structure of the active layer also changes its sensitivity. **Table 2** shows an example of a change in sensitivity (glucose) with a change in the morphology of ZnO-based nanostructures [18].

As for the sensitive layer, the choice of the biosensor substrate material is an important factor. The choice of material as a porous silicon for the matrix is due to a wide range of key qualities required by structures for an effective use in biomedicine. These are the simplicity for functionalization, the ability to control the morphology and surface composition of porous matrices, the low cost of production, functional "flexibility," and good compatibility with the current industrial technologies. As a result, the porous silicon matrix can serve as the basis for composite structures. High values of surface area and specific area allow functionalization using a variety of biocompatible materials (silver, gold, magnetic metals, iron groups, tin, indium, zinc and their oxides).

The development of highly sensitive blood glucose meters is an extremely important task. This is especially important in the direction of personalized medical devices for people with diabetes. A promising task is the creation of noninvasive highly sensitive sensors with a low detection limit (of the order of 0.1 μM or less) [19–21]. The lower the detection limit parameter, the earlier a change in glucose level can be detected. These detection limit values can be achieved by using porous semiconductors as a substrate. It should be noticed that the morphological features of porous structures make it difficult to create a high-quality electrode base. To solve this problem, new methods have been developed for the functionalization of porous matrices with the aim of active deposition of nanoparticles into pores. The developed methods are non-destructive in comparison with analogues. The creation of a high-quality electrode base, with a large specific area of the sensitive layer, a high sensitivity parameter, a small detection limit, and small device sizes, is key to creating new personalized glucometers for recording glucose changes in direct time.

Thus, this work, the purpose of which is to study the physicochemical, electrical, and optical properties, as well as the morphological features of porous

Sensor type	Sensitivity
Glucose sensor based on Pd/WO_3-ZnO composite porous thin films	11.4 μA μM^{-1} cm^{-2}
Glucose biosensors with AuNPs (glassy carbon electrode (GCE) + AuNPs)	3.1 μA mM^{-1} cm^{-2}
Glucose biosensors based on GQDs	0.085 μA μM^{-1} cm^{-2}
Glucose biosensors based on Ag/TiO2 composite	39 μA mM^{-1} cm^{-2}
Glucose biosensors based on **c**arbon nanotube	1433 μA mM^{-1}·cm^{-2}
Glucose biosensors based on ZnO nanoparticles	15 mA mM^{-1}·cm^{-2}

Table 1.
Sensitivity data for various types of biosensors during glucose recording [6–17].

Type of structures	Sensitivity
ZnO nanowire	26.3 mA mM^{-1} cm^{-2}
ZnO nanocomb	15.33 μA mM^{-1} cm^{-2}
ZnO:Co nanocluster	13.3 μA mM^{-1} cm^{-2}
Pyramid-shaped porous ZnO	237.8 μA mM^{-1} cm^{2}

Table 2.
Sensitivity of ZnO nanostructures with different morphology [18].

silicon matrices with varying technological parameters for the preparation of substrates and methods for their functionalization, is relevant and is of scientific and practical interest.

2. The formation of porous silicon matrices by electrochemical etching under various conditions

2.1 Method for the formation of porous silicon matrices

For the formation of a porous matrix, the method of electrochemical etching in aqueous solutions of hydrofluoric acid was used. A detailed installation diagram is presented in **Figure 1**. The structure of the stand can be divided into separate components: a glassy carbon crucible which contains electrolyte (1), a silicon wafer (2), and devices used to move the crucible and the sample in different planes (3)–(5).

During the electrochemical process, silicon atoms actively react with the molecules (ions) of the electrolyte when they come into solution. This process was formulated by Lehman and Joselle, describing the migration of holes at the surface of a sample when a current is applied. Therefore, it is worth considering that such etching modes as current density and anodization time directly affect the structure of the porous layer. The composition of the electrolyte also affects the morphology of the matrix. In this work an aqueous solution of hydrofluoric acid with the

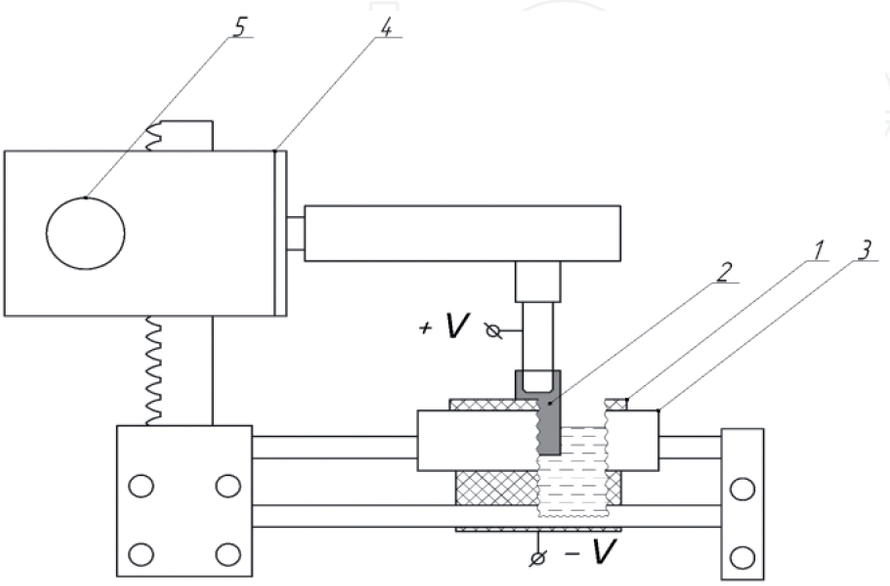

Figure 1.
Installation for electrochemical etching: (1) crucible; (2) sample; (3) platform; (4) carriage; and (5) height adjustment knob.

addition of isopropyl alcohol (C_3H_7OH) was used. This solution provides the necessary wettability of the silicon wafer surface by electrolyte [22–25].

As a result of electrochemical etching, observing the galvanostatic mode (current density j = 30 mA/cm^2: anodizing time t = 10 min), porous substrates were formed. New structures were subsequently used as the basis for the formation of por-Si/Ag and por-Si/ZnO composite structures.

2.2 Functionalization methods

To create functionalized composite structures, Ag nanoparticles were deposited on the formed porous substrates. Also, under an electrothermal influence, it was possible to ensure the diffusion of nanocrystals into the matrix. These functionalization methods allow the formation of composites with new structural and physicochemical properties.

2.2.1 Synthesis of silver nanoparticles using silver nitrate ($AgNO_3$)

In this work, silver ink using the recovery method with sodium citrate and with the addition of a strong reducing agent, which allows one to achieve the necessary concentration of supersaturation in the early stages of synthesis, was obtained [26]. Ascorbic or tannic acid can act as a strong reducing agent.

The solution is formed by heating for 30 min a mixture based on silver nitrate, sodium citrate and sodium chloride, and a solution of ascorbic acid heated to 95°C is added. Then, unreacted components are removed from the solution by centrifugation. Subsequently, in several stages, silver layers were applied followed by annealing at a temperature of 150°C for 30 min.

To determine the sizes of the synthesized silver nanoparticles, the scanning electron microscopy (SEM) method was used (**Figure 2**).

Based on the obtained images, it was concluded that the diameter of silver nanocrystals is about 20 nm.

2.2.2 Functionalization method based on the electrochemical deposition of zinc oxide nanoparticles

In this work, the functionalization of zinc oxide nanoparticles with porous silicon samples was carried out using the electrochemical deposition of metals from an electrolyte solution [27]. For this methodology an installation was developed as shown in **Figure 3**.

The electrodeposition was carried out as follows: in a crucible (6) with electrolyte (5), which was previously heated to a temperature of 65°C, a previously prepared sample of a porous silicon (4) was immersed. An electric current in the range from 0.5 to 1 A was passed through anode (6) and cathode (3), which provided the beginning of the electrodeposition process. Motor (2) provided a continuous mixing of the electrolyte solution during electrodeposition at a speed of 5000 r/s for 1 h. Then, the samples of porous silicon with a deposited layer of zinc were annealed in a muffle furnace at a temperature of 200°C for 20 min.

2.2.3 Functionalization method based on electrothermal diffusion processes

To ensure a high-quality introduction of silver nanoparticles into porous matrices, the method of electrothermal diffusion was used. Installation for the implementation of this process is presented in **Figure 4**.

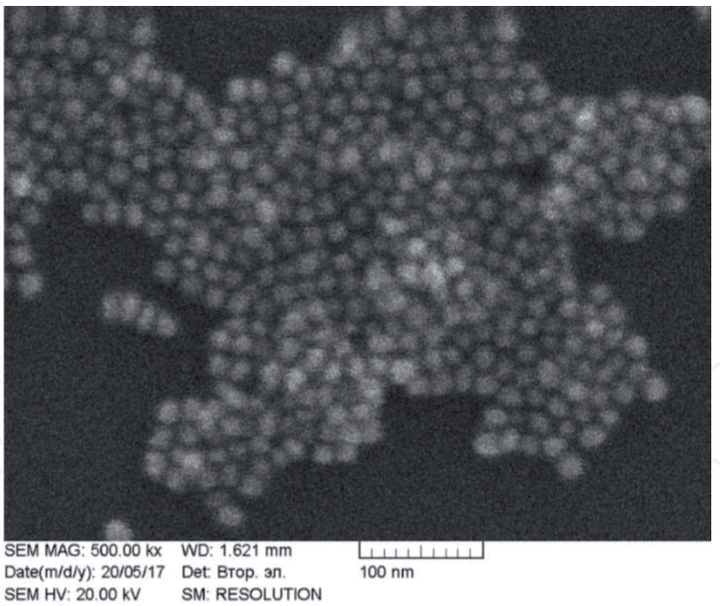

Figure 2.
Image of synthesized silver nanoparticles.

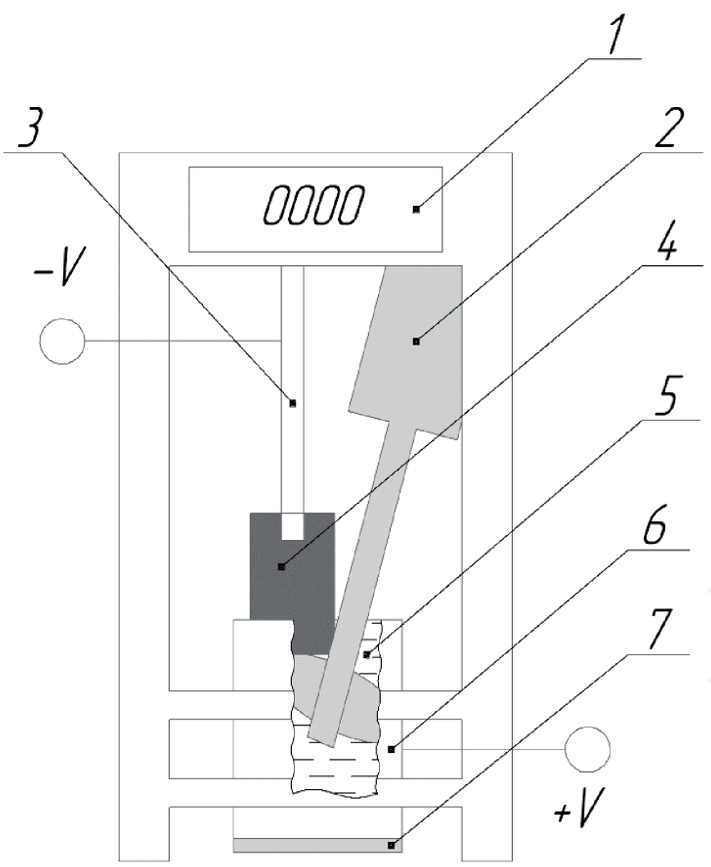

Figure 3.
Installation for electrodeposition of metals: (1) indicator of motor rotation speed; (2) motor; (3) cathode; (4) sample (to which electrodeposition is performed); (5) electrolyte; (6) graphite crucible (anode); and (7) heating element (Peltier element).

This installation includes a muffle furnace (1) (capable of maintaining a temperature of up to 900°C) with a fixed sample on the worktable. The clamping mechanism (acting as the anode) fixes the sample and implements the current to the surface layer.

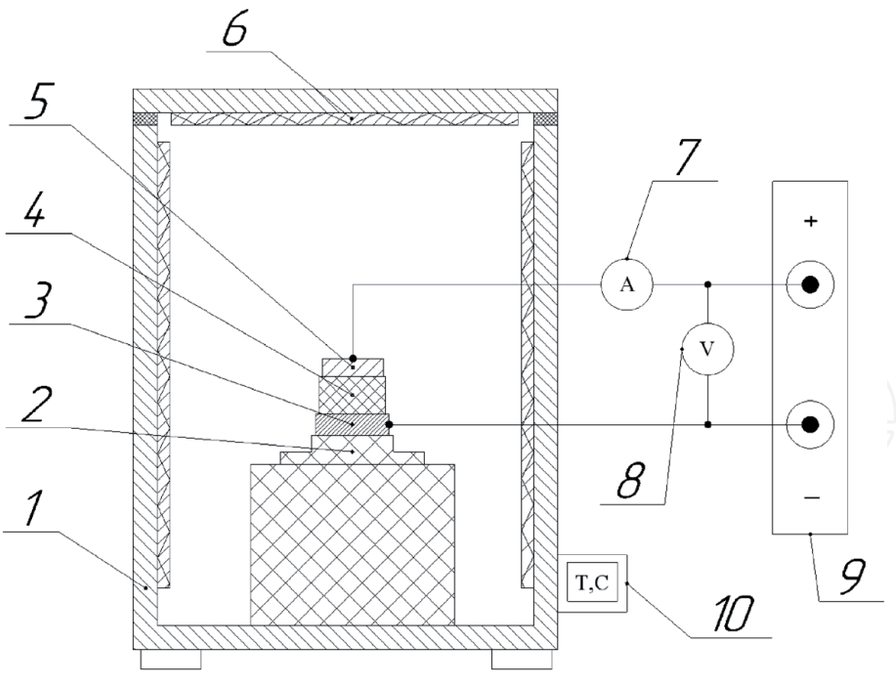

Figure 4.
Installation for functionalization by electro (E)-diffusion method: (1) muffle furnace; (2) desktop; (3) a metal film (cathode); (4) porous semiconductor; (5) metal layer (anode); (6) heaters; (7) milliammeter; (8) voltmeter; (9) power supply; and (10) thermometer.

Samples, on which silver layers were deposited by the method of colloidal quantum dots, were fixed on the worktable. Then, the table was placed in a muffle furnace and preheated to 200°C for 15 min. This process is necessary to avoid thermal shock and prevent the destruction of the material. To activate electro-diffusion, a voltage of 300 V was applied to the samples. This electrothermal process was observed for 25 min. Then, the voltage supply stopped and the samples are cooled for 30 min inside the furnace. Using this method a series of samples in which silver nanoparticles diffused deep into the porous matrix were obtained. The thermal deposition of metals into the porous layer took place at the same parameters as the deposition by electrothermal diffusion, but without applying an electric potential to the sample [28–30].

3. Assessment of the morphology of nanostructures using SEM methods

In this work, the samples formed during the experiments were studied by scanning electron microscopy (TESCAN MIRA3 electron microscope). This technique allowed us to determine the morphological features of porous matrices before and after functionalization processes. The measurement results are presented in **Figures 5–9**.

Based on the obtained images (**Figure 5**), it was concluded that the size of pores for por-Si matrices is about 50 nm and the thickness of the porous layer is 20 μm. **Figure 6** shows the images for porous silicon matrices after the functionalization process (deposition of silver nanoparticles by the method of colloidal quantum dots).

The layered deposition of silver nanoparticles allows to achieve good uniformity on the surface of the substrate. Also, according to the data obtained (**Figure 6**), it was found that silver is predominantly localized on the porous matrix and only a small fraction goes deep into the wide pores. **Figure 7** shows SEM images of samples coated with a layer of silver after the electro-diffusion process.

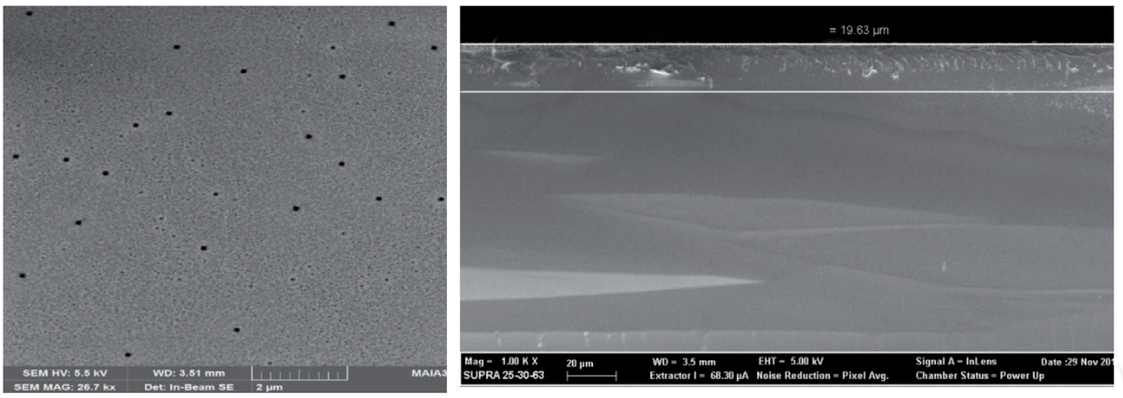

a) b)

Figure 5.
Scanning electron microscopy data of a porous silicon matrix: (a) surface and (b) cross section.

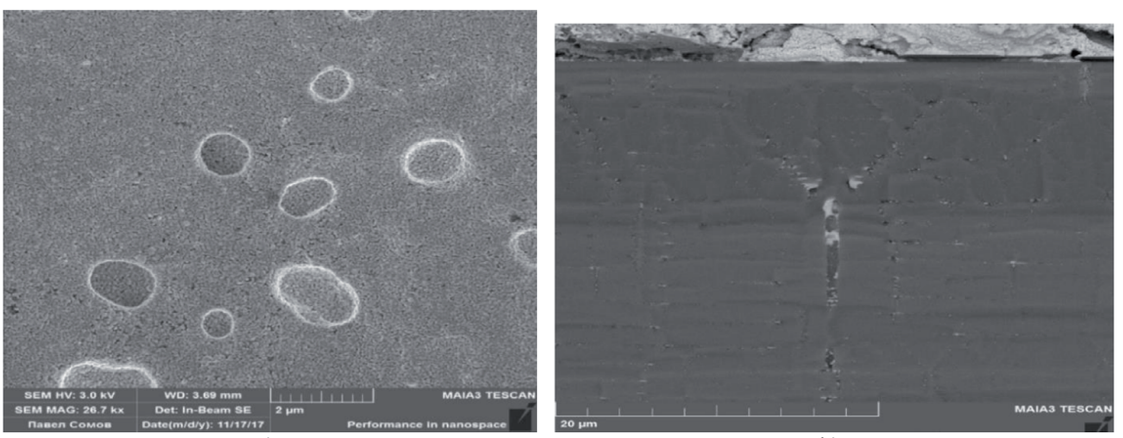

a) b)

Figure 6.
Scanning electron microscopy data of por-Si/Ag structures: (a) surface and (b) cross section.

==

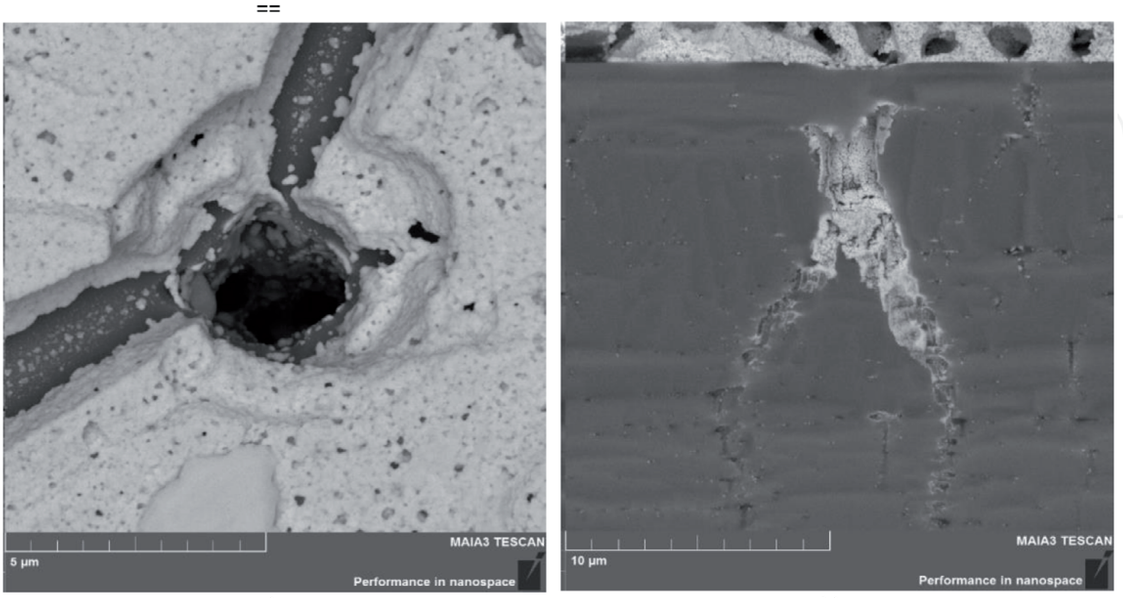

a) b)

Figure 7.
SEM data of por-Si/Ag structures after the process of electro-diffusion: (a) surface and (b) cross section.

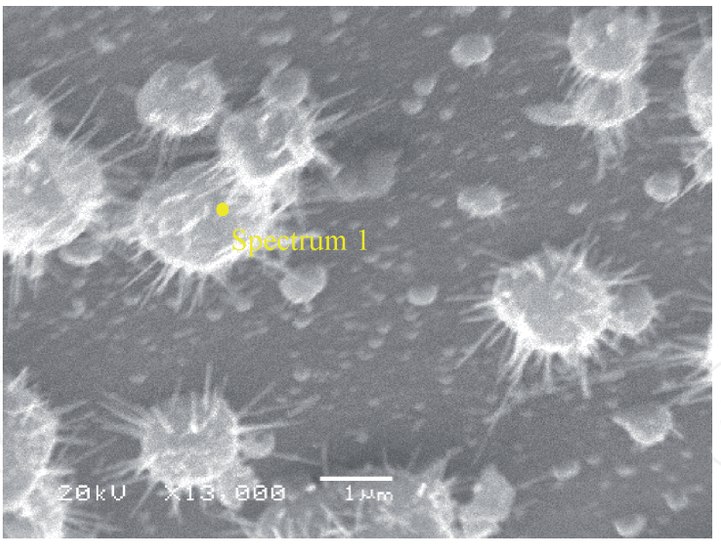

Figure 8.
SEM data of the por-SI/ZnO structure.

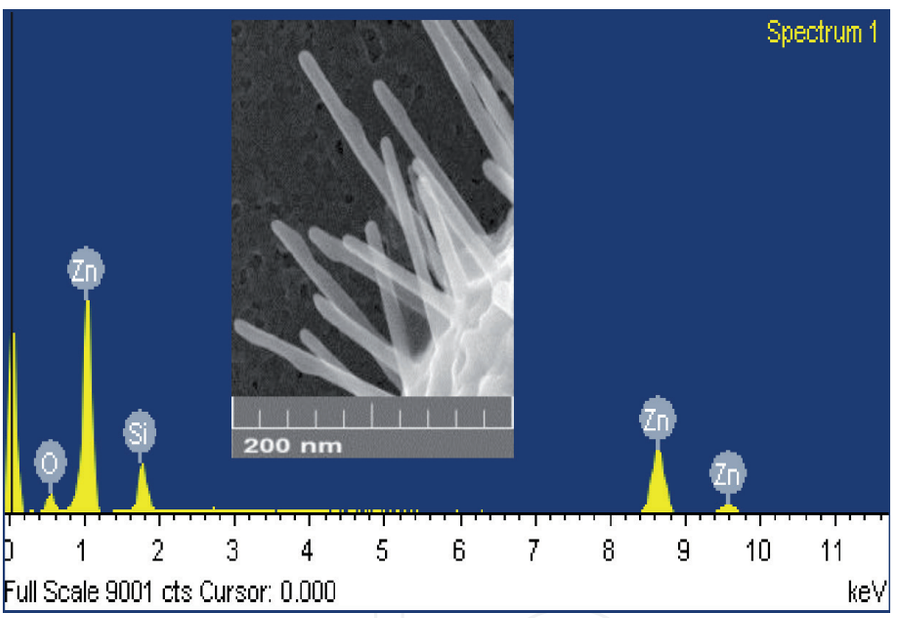

Figure 9.
EDX analysis of por-Si/ZnO structure.

It was found (**Figure 7**) that after the functionalization process based on electrodiffusion, silver actively diffuses into the pores. The combined effect of the electric and thermal conditions ensures the activation of this process. Unlike conventional layering, silver nanoparticles occupy almost the entire pore depth.

3.1 Study of composite structures por-Si/ZnO by SEM method

To study the por-Si/ZnO composite structures, scanning electron microscopy (TESCAN MIRA3 microscope) was used. Also energy-dispersive X-ray spectroscopy (EDX) to analyze the composition was used. The data are presented in **Figures 8** and **9**.

In **Table 3** the EDX analysis data described in **Figure 9** is presented.

Thus, it was found that zinc particles predominate in the studied structures. The mass fraction of Zn is 77.83% of the total mass of por-Si/ZnO. It can be argued that

Element	Mass, %	Atom content, %
O K	10.51	29.03
Si K	11.66	18.35
Zn K	77.83	52.62
Total	100	100

Table 3.
EDX data analysis.

during the electrochemical deposition of zinc oxide nanoparticles, the active passivation of the porous surface occurs, followed by the oxidation of the nanoparticles. Also based on SEM data, it was concluded that the largest ZnO nanoparticle size reaches about 2 μm. The size of the rods in this case varies in the range from 200 nm to 1 μm. These particles are formed on the surface of the porous matrix, fixing on its surface.

4. The study of composite structures by IR and Raman spectroscopy

4.1 The study of composite structures by IR spectroscopy

The IR transmission spectra of the samples were obtained on a Vertex 70 FTIR spectrometer (Bruker) using an attachment for spectroscopy of impaired total internal reflection (TIR) [31]. The depth of study of porous silicon samples by wavelengths up to 2000 cm^{-1} does not exceed 1.5 μm by this technique, and in the range of 2000–4000 cm^{-1}, it does not exceed 10 μm. Thus, based on our calculations and the data on the thickness of the porous layers obtained using SEM, by the ATR method, we obtain data mainly on the composition of the porous layer with an insignificant contribution from the substrate. IR spectra were obtained a month after the manufacture of the samples (**Figure 10**).

According to IR spectroscopy, after 30 days of exposure to the atmosphere, the spectrum of a "standard" por-Si sample shows bands characteristic of porous silicon, corresponding to Si-Si and Si-H bonds (616 and 634 cm^{-1}); band 750–1000 cm^{-1}, corresponding to different types of Si-H and O_xSi_y bonds; the oxide compound peak of Si-O-Si (1060–1250 cm^{-1}); and the band 2150–2250 cm^{-1}, corresponding to various types of vibration of bonds of adsorbed hydrogen and oxygen-containing groups [32]. In addition, the band at 480 cm^{-1} of the spectrum corresponds to deformation vibrations of Si-O-Si.

The spectra of porous silicon samples with deposited silver nanoparticles were uninformative, apparently, due to the high reflectivity of the formed silver film. No pronounced absorption bands were observed on the spectra of these samples by this technique.

The situation is different for por-Si samples with various methods of functionalization (electro-, thermo-, and electrothermodiffusion methods) of ZnO films. The deposition of zinc oxide on the surface leads to a change in the degree of oxidation of the surface, a decrease in the intensity of the band of the oxide composite peak of Si-O-Si stretching vibrations (1060–1250 cm^{-1}), and a characteristic of stoichiometric silicon dioxide (SiO_2) with an increase in the intensity of the absorption peak corresponding to Si-O deformation vibrations—Si. The band corresponding to Si-Si bonds also becomes less pronounced against the background of an increase

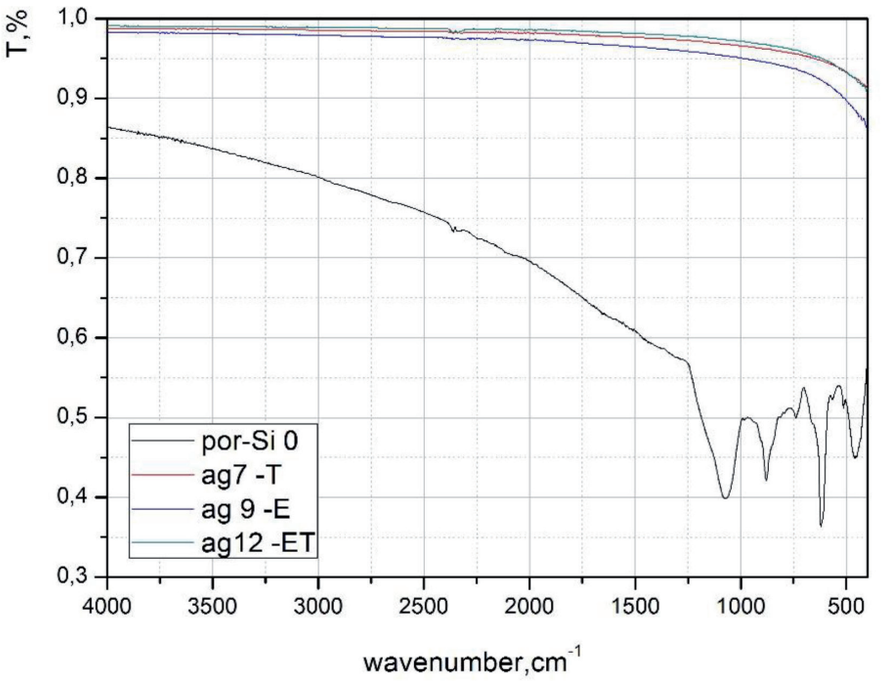

Figure 10.
IR transmission spectra of samples of porous silicon with deposited silver functionalized by electro-, thermo-, and electrothermodiffusion (E-T) methods.

in the intensity of the complex compound band of 750–1000 cm^{-1}, corresponding to various types of Si-H and O_xSi_y bonds. A change in the shape of the absorption band of the spectrum of 750–1000 cm^{-1} shows that the deposition of zinc oxide leads to a decrease in the fraction of Si-H_x bonds on the surface of the porous layer and a corresponding increase in oxygen-containing bonds of the O_xSiH_y type. Comparing the samples of porous silicon with ZnO functionalized by different methods, we can conclude that, with the general tendency toward a change in the oxidation state of porous silicon described above, the electrical effect of zinc oxide affects the por-Si surface to a lesser extent than thermal and electrothermal effects (**Figures 11** and **12**).

Comparing the samples of porous silicon with deposited ZnO functionalized by different methods, we can conclude that, with the general tendency toward a change in the oxidation state of porous silicon described above, the thermal deposition of zinc oxide affects the por-Si surface to a lesser extent compared to electrically and electrothermally modified.

4.2 The study of composite structures by Raman spectroscopy

Raman spectra (Raman light scattering) were recorded in the backscattering geometry at room temperature using a Raman Microscope RamMics M532 EnSpectr laboratory Raman spectrometer. As an excitation source, a 532 nm Nd:YAG laser was used. The Raman spectroscopy method was used as an addition to the IR spectroscopy method to determine the effect of metal film deposition on post-processing on the composition of the matrix of porous silicon. The estimated depth of analysis by this technique was about 1 μm.

The Raman spectrum of porous silicon has the same features as the spectrum of the crystalline silicon substrate on which it was grown. However, the spectrum of porous silicon broadened the main band corresponding to the TO-phonon line of silicon (520.7 cm^{-1}), as well as more pronounced features at 300 (LA phonon of silicon)

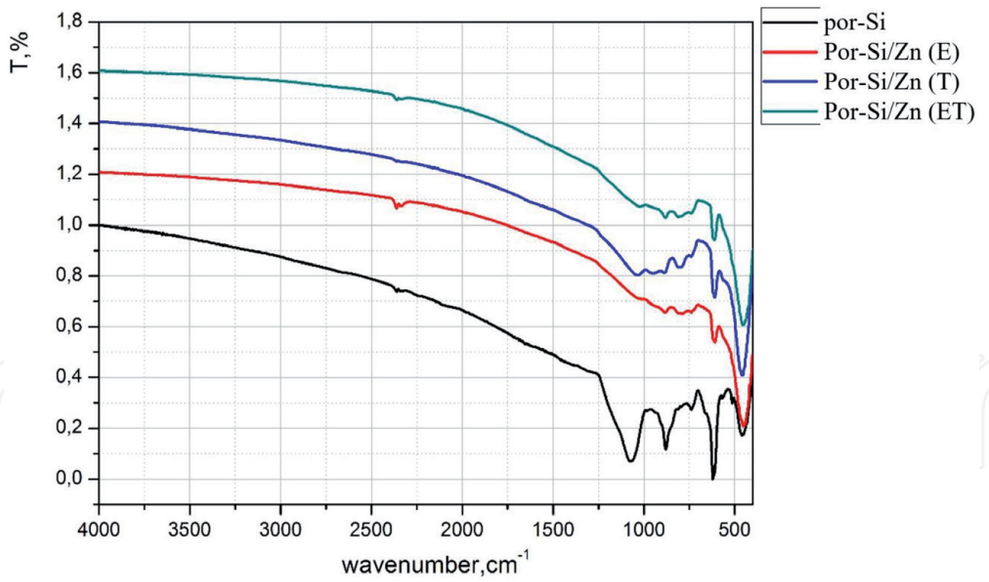

Figure 11.
IR transmission spectra of samples of porous silicon with zinc oxide layers functionalized by the methods of electro-, thermo-, and electrothermodiffusion methods.

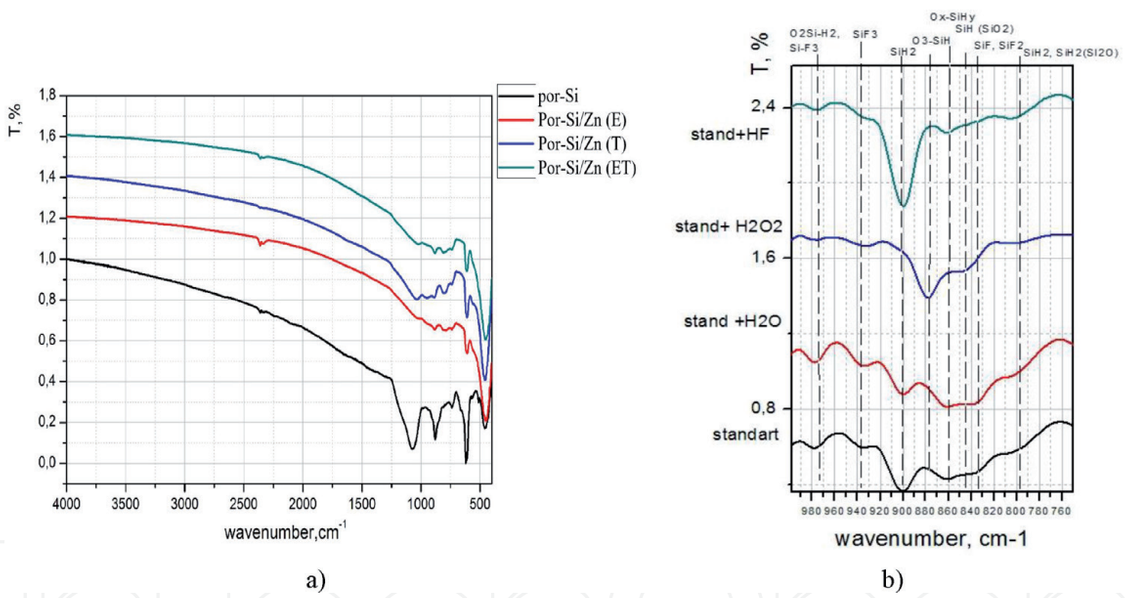

Figure 12.
(a) IR transmission spectra of samples of porous silicon with deposited zinc oxide nanoparticles functionalized by electro-, thermo-, and electrothermodiffusion methods, the spectral region is 760–1500 cm^{-1}. (b) An example of deciphering the features of the IR spectrum of porous silicon samples in the region of 760–960 cm^{-1} according to [32].

and 950–1000 cm^{-1} (TO-phonon, second order). The broadening of the main band and the increase in the intensities of the minor bands of the Raman spectrum can be explained by the structural deformations of silicon during the formation of pores in it (**Figures 13** and **14**).

It was found that the deposition of silver and zinc oxide into porous silicon does not significantly affect the shape of the spectrum of porous silicon. In this case, however, a slight broadening of the main band of the TO-phonon of silicon occurs, which indicates a slight additional deformation of the porous matrix; moreover, a wide band of 1200–1600 cm^{-1} appears on the Raman spectra of the samples with deposited metals, which corresponds to carbon contamination of the surface by the deposition products (amorphous carbon).

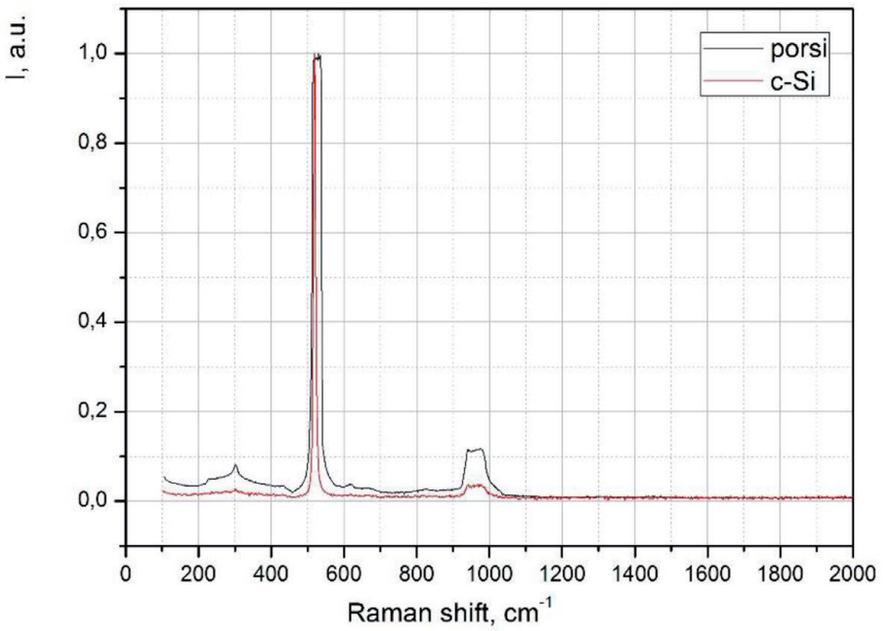

Figure 13.
Normalized Raman spectra of porous silicon samples and c-Si substrates.

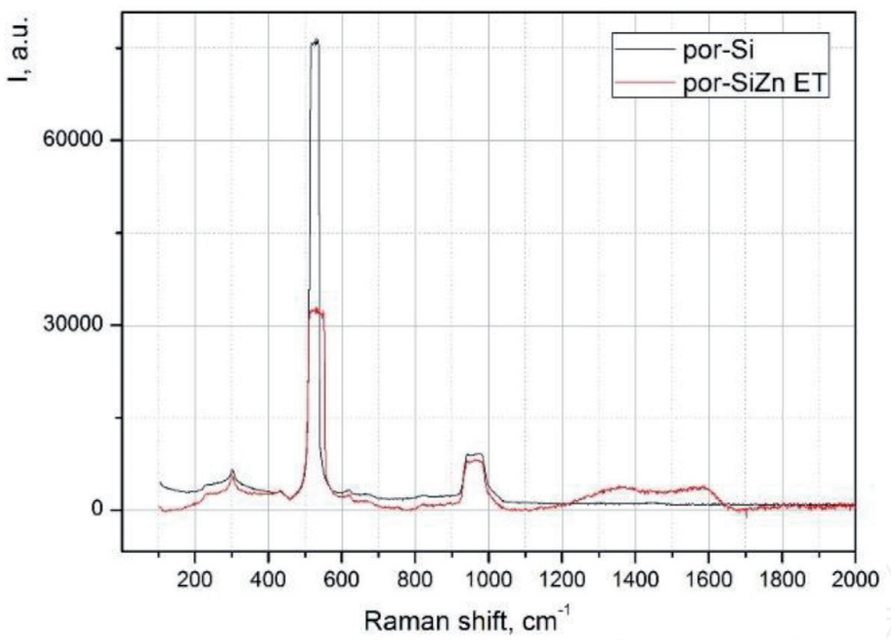

Figure 14.
Raman spectra of the samples por-Si and por-Si/Zn under an electrothermal diffusion effect.

5. The study of samples using an ultrasoft X-ray emission spectroscopy

X-ray emission USXES Si L2,3 spectra of the samples were obtained on a unique laboratory X-ray spectrometer-RSM-500 monochromator, in high vacuum (3×10^{-6} mmHg); the energy resolution of the obtained spectra was 0.3 eV. This technique is sensitive to the local partial density of states of atoms of a certain sort, due to which a qualitative assessment of the atomic structure of porous silicon and a semiquantitative assessment of the relative phase content in this material are possible [33]. In the case of porous silicon, USXES Si L 2,3 spectra reflect the distribution of Si 3S + Si 3d states with a predominance of Si 3 s. The depths of analysis by this method were ~30 and 60 nm at an accelerating voltage at the anode of the X-ray tube, on which the test sample was placed, 2 and 3 kV, respectively.

The obtained X-ray emission spectra were processed using a special computer program, which allows the phase composition of the obtained por-Si samples to be determined by summing the spectra of reference materials with the corresponding weight coefficients that can be part of the porous layer [33]. When simulating the Si L 2,3 spectra of por-Si samples, the following reference spectra were used: single-crystal silicon (c-Si); amorphous hydrogenated silicon (a-Si:H); low-coordinated (lc) silicon Si, which was observed in amorphous Si films [34] (coordination number ~2.5–3); disordered silicon after implantation with argon Si:Ar; silicon suboxide (SiOx), where x is 1.3; and SiO_2 [34, 35]. The modeling error was determined as the difference between the areas under the experimental and simulated Si L 2,3 spectra and did not exceed 10%. In addition the general form of the simulated and experimental spectra was taken into account [36]. The survey was carried out 1 month after receiving the samples (**Figure 15**).

Figures 16 and **17** show the USXES Si L2,3 spectra of samples of the initial porous silicon and porous silicon with deposited silver and zinc oxide nanoparticles, obtained for the analysis depths of 30 (a) and 60 (b) nm.

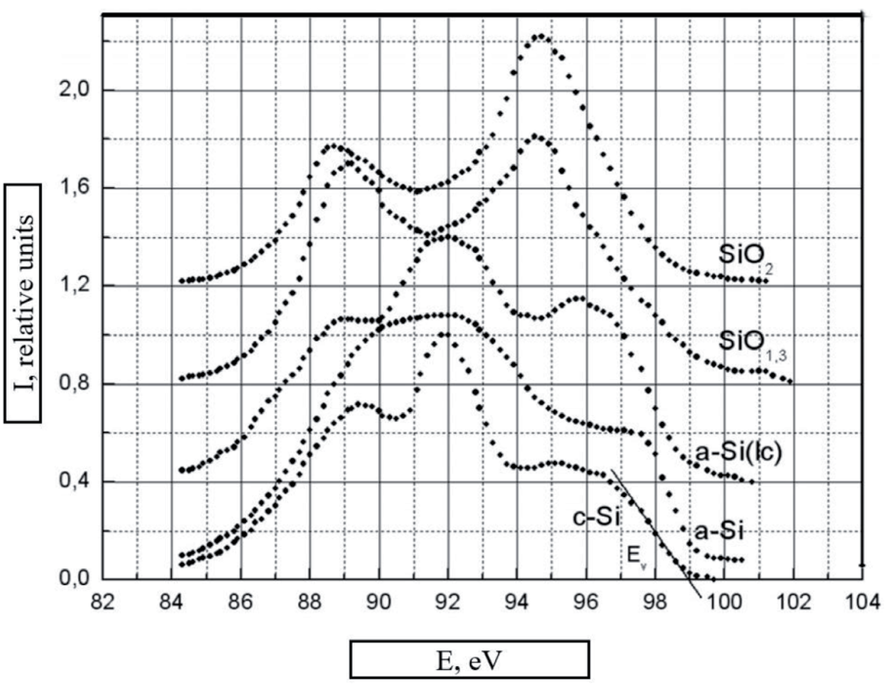

Figure 15.
USXES Si L2,3 spectra of reference phases.

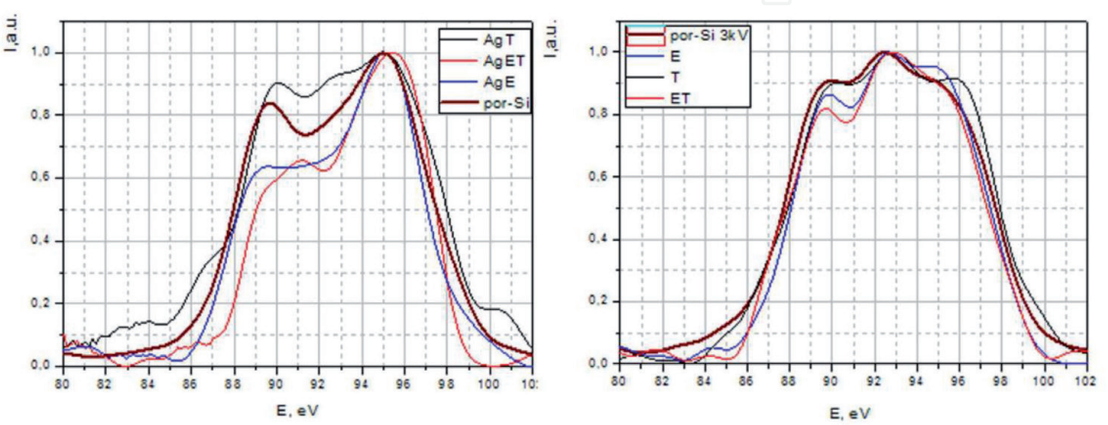

Figure 16.
USXES Si L2,3 porous silicon and por-Si with deposited silver nanoparticles.

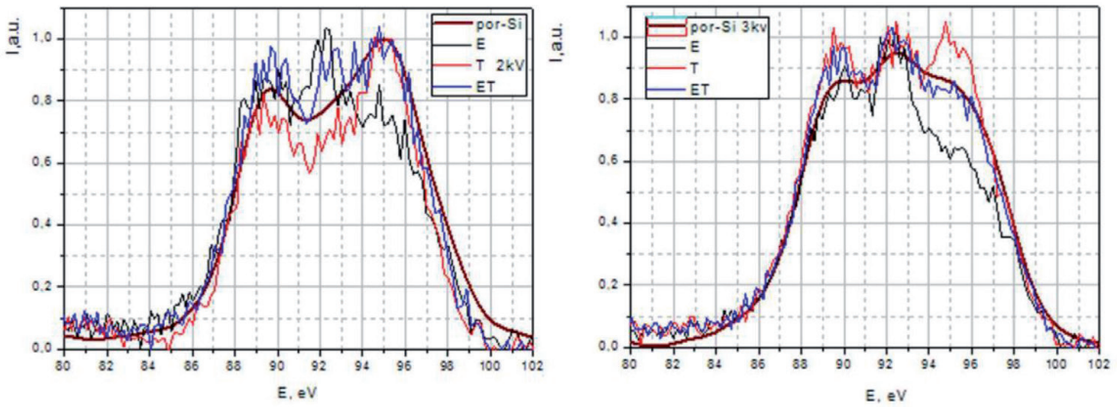

Figure 17.
USXES Si L2,3 porous silicon and por-Si with deposited ZnO nanoparticles.

At an analysis depth of 30 nm by the USXES method, the following data were obtained. The closer to the surface layer of the initial porous silicon is predominantly oxidized, the fraction of unoxidized silicon (c-Si, a-Si) on the surface is less than 50% (burst 10%), while por-Si/Ag substrate functionalized by the electrical and electrothermal methods leads to stronger oxidation matrices predominant in the surface composition of SiO_2 oxide. Thermal method of modification has a lesser effect on the surface composition of the porous silicon matrix used, while the fraction of unoxidized phases in the surface composition slightly increases. This can be attributed to the morphological features of the film grown on the surface by this technique.

With a greater depth of analysis by the USXES method, at 60 nm, the following data were obtained: the phase composition of more porous silicon is expectedly less oxidized compared to its surface; the contribution of crystalline and amorphous silicon phases prevails over the contribution from oxide phases. In this case, the por-Si/Ag samples functionalized by all methods have a significantly smaller effect on the composition of the por-Si matrix layer deeper; phase analysis shows approximately the same ratio of oxidized and non-oxidized phases as in the initial porous silicon with a slight increase in the oxidation state, i.e., defective SiOx is oxidized to SiO_2, while maintaining the proportion of SiOx + SiO_2 in the total phase composition.

The following data were obtained for composites with precipitated ZnO at an analysis depth of 30 nm using the USXES method. Recall that we used the same matrix of porous silicon in the same series of samples. As in the case of the deposition of silver nanoparticles, the functionalization of zinc oxide structures by the thermal method has the least effect on the surface composition of the porous silicon matrix used (toward a slightly higher matrix oxidation). This can be attributed to the morphological features of the film grown on the surface by this technique. The functionalization of ZnO particles by electro- and electrothermal diffusion methods leads to a stronger change in the composition of the matrix surface, namely, a significantly smaller contribution of silicon oxide phases, with the most pronounced changes observed in samples with ZnO electrochemical modification.

With a greater depth of analysis by the USXES method, at 60 nm, the following data were obtained: the most pronounced changes in the phase composition, as well as at a shorter depth of analysis, are observed in samples with por-Si/ZnO samples with electrical modification; the degree of oxidation of the porous layer in these samples is significantly lower than the initial porous silicon. In electrothermal and thermal functionalization, the most severe changes which are observed in por-Si/ZnO samples with electrical modification to a lesser extent affect the composition of the matrix, leading to a slight increase in the fraction of oxide phases.

6. The study of the photoluminescent characteristics of samples

The photoluminescent (PL) spectra of multilayer porous silicon were measured using an experimental setup based on an OceanOptics USB4000-VIS–NIR (350–1000 nm) optical fiber spectrometer. An HP Lightning light-emitting diode (LED) was used as the PL excitation source, the maximum radiation wavelength of which was 405 nm (~3.06 eV). A quartz-focusing lens and a band-pass filter were installed in front of the LED, cutting out the long-wavelength region of the LED's radiation. The PL radiation of the samples was introduced into the QP600–2-UV–VIS (OceanOptics) fiber through a collimator. Next, the radiation was directed to the input of the spectrometer. The measurements were carried out in the dark in the absence of scattered light sources a month after the preparation of the samples.

The photoluminescence spectrum of the initial porous silicon is a band in the region of 500–800 nm with a peak of ~650 nm and is a characteristic of por-Si samples obtained by this method. The deposition of silver nanoparticles using

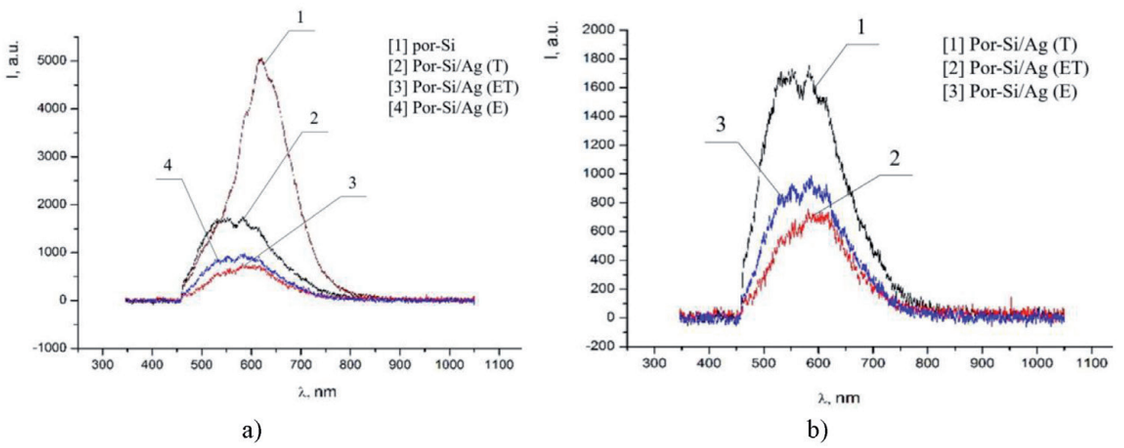

Figure 18.
PL spectra of samples of porous silicon and porous silicon with deposited silver nanoparticles with different types of functionalization; a) full spectra for all samples, b) local part of the spectrum: (por-Si) - porous silicon, (por-Si/Ag (T)) porous silicon with Ag nanoparticles functionalized by thermal exposure, (por-Si/Ag (E)) porous silicon with Ag nanoparticles functionalized by electrical exposure, (por-Si/Ag (ET)) porous silicon with Ag nanoparticles functionalized by electrothermal exposure.

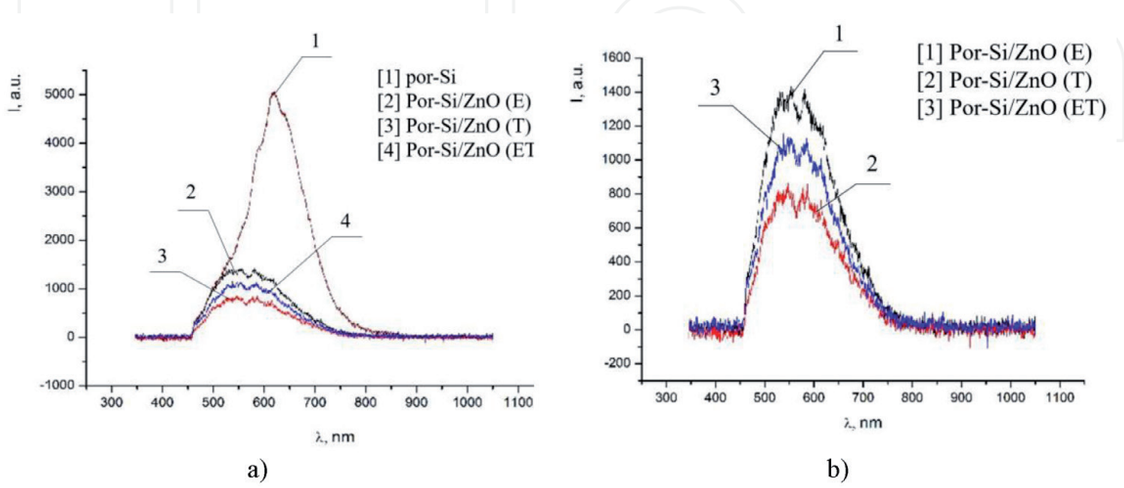

Figure 19.
PL spectra of samples of porous silicon and porous silicon with deposited ZnO nanoparticles with different types of functionalization; a) full spectra for all samples, b) local part of the spectrum: (por-Si) - porous silicon, (por-Si/ZnO (T)) porous silicon with ZnO nanoparticles functionalized by thermal exposure, (por-Si/ZnO (E)) porous silicon with ZnO nanoparticles functionalized by electrical exposure, (por-Si/ZnO (ET)) porous silicon with ZnO nanoparticles functionalized by electrothermal exposure.

the techniques used in this work leads to a noticeable shift of the PL peak toward shorter wavelengths with a slight decrease in the PL intensity. The peak of the PL of samples with por-Si/Ag samples modified by various techniques is in the region of 550–600 nm, with the highest PL intensity having the composite sample functionalized by thermal exposure (**Figures 18** and **19**).

The deposition of zinc oxide nanostructures by the methods used in this work, as in the case of deposition of silver nanoparticles, leads to a noticeable shift of the PL peak toward shorter wavelengths with a slight decrease in the PL intensity. The peak of the PL of por-Si/ZnO samples functionalized by various techniques is in the range of 550–600 nm, with the highest PL intensity having the composite sample modified by electrical exposure.

7. Conclusions

1. There were a series of porous silicon substrate by electrochemical etching obtained. To create functionalized composite structures, Ag and ZnO nanoparticles were deposited on the formed porous substrates. Silver ink was formed by reducing sodium citrate at high supersaturation concentrations. Zinc oxide nanoparticles were deposited on substrates by electrochemical deposition of metals from an electrolyte solution. To ensure the effective introduction of silver and zinc oxide nanoparticles into the porous matrix, the method of electrothermal diffusion was used.

2. There were obtained data by scanning electron microscopy for all series of samples. Based on the analyzed images, it was concluded that the porous silicon substrate pore size is about 50 nm and the thickness of the porous layer 20 μm. When silver nanoparticles are deposited on a porous matrix, localization is achieved mainly on the surface of the substrate. By the method of electrothermal diffusion of the nanoparticle, active diffusion of particles deep into the pores was achieved. Silver actively diffuses into the pores, occupying almost the entire pore depth. Thus, SEM made it possible to estimate the particle size of ZnO reaching up to 2 μm (rod lengths in the range from 200 nm to 1 μm). Particles of such sizes do not penetrate into the pores and remain fixed on the surface of the porous matrix.

3. There were obtained data on the surface composition of nanostructures by IR and Raman spectroscopies. The IR transmission spectra of the samples were detected on a Vertex 70 FTIR spectrometer (Bruker). An analysis of the spectra indicates that the exposure of the samples in the atmosphere activates the oxide compound peak Si-O-Si (1060–1250 cm^{-1}). Also, on the spectra there is a band at 480 cm^{-1} corresponding to deformation vibrations of Si-O-Si.

   Due to the high reflectivity of the silver layer, it was not possible to reveal pronounced absorption bands in the spectra. In this case, the obtained data for por-Si/ZnO composite structures led to the conclusion that the deposition of a zinc oxide layer on the substrate leads to a change in the oxidation state of the surface, which leads to a decrease in the intensity of the oxide composite peak band of Si-O-Si stretching vibrations (1060–1250 cm^{-1}). The spectra showed changes in the shape of the absorption band of the spectrum of 750–1000 cm^{-1}. This fact indicates a decrease in the fraction of Si-Hx bonds and a corresponding increase in oxygen-containing bonds of the OxSiHy type when silver nanoparticles are deposited on the substrate surface.

4. By the method of ultrasoft X-ray emission spectroscopy, data on the atomic and electronic structures and phase composition of the nanostructures were obtained. USXES X-ray emission spectra indicate that the porous matrix is primarily predominantly oxidized by a, the fraction of unoxidized silicon (c-Si, a-Si) on the surface is less than 50% (burst 10%), while the deposition of silver nanoparticles leads to stronger oxidation of the matrix, the prevalence of SiO_2 oxide in the surface composition. In this case, an increase in the fraction of unoxidized phases in the surface composition is observed.

   For composite structures based on por-Si/ZnO and por-Si/Ag, the USXES method was used to analyze the phase composition at various depths of 30 and 60 nm. For both types of composite matrices, temperature oxidation at depths of 30 nm and 60 nm results in the oxidation of the active surface, but the overall composition remains almost unchanged. It should be noted that during the functionalization of composite structures by the methods of electro- and electrothermodiffusion, a significant change in the composition of the surface layer occurs as a result of diffusion processes. A significant decrease in the oxide phases of silicon was also noted.

5. The photoluminescent characteristics of the samples were investigated using a USBO4000-VIS–NIR fiber-optic spectrometer (350–1000 nm) from Ocean-Optics (the maximum radiation wavelength of which was 405 nm (~3.06 eV)). When studying the spectra of substrates, characteristic spectra were obtained for this type of porous matrices (a band in the region of 500–800 nm with a peak of ~650 nm). The functionalization of the surface by silver nanoparticles leads to a noticeable shift of the PL peak toward shorter wavelengths with a slight decrease in the PL intensity. The electrical, thermal, and combined effects are determined on the PL spectra by a peak in the region of 550–600 nm, while the composite structure corresponding to the thermal effect has the highest PL intensity.

   The deposition of zinc oxide nanostructures by the methods used in this work, as in the case of deposition of silver nanoparticles, leads to a noticeable shift of the PL peak toward shorter wavelengths with a slight decrease in the PL intensity. The PL peak of samples with ZnO nanostructures deposited by various techniques is in the range of 550–600 nm. Unlike por-Si/structures, the highest PL intensity has a sample that was subjected to electrothermal interaction.

6. The main results of this work include the data obtained during the study, which allow to determine the patterns of influence of the presented functionalization modes on the characteristics of porous matrices. The studied structures can be used as sensory devices with an increased level of sensitivity and have a wide range of detectable analyses.

Author details

Veniamin Koshevoi[1*], Anton Belorus[2], Ilya Pleshanov[3], Anton Timchenko[4], Roman Denisenko[3], Daniyar Sherimov[2] and Ekaterina Vodkailo[1]

1 St. Petersburg Mining University, Saint-Petersburg, Russia

2 St. Petersburg Electrotechnical University "LETI", Saint-Petersburg, Russia

3 St. Petersburg National Research University of Information Technologies, Saint-Petersburg, Russia

4 Immanuel Kant Baltic Federal University, Kaliningrad, Russia

*Address all correspondence to: venia.koshevoi.eltech@gmail.com

References

[1] Leigh C. Handbook of Porous Silicon. 2nd ed. Switzerland: Springer International Publishing; 2014. p. 1613. DOI: 10.1007/978-3-319-05744-6

[2] Yin J, Qi X, Yang L, Hao G, Li J, Zhong J. A hydrogen peroxide electrochemical sensor based on silver nanoparticles decorated silicon nanowire arrays. Electrochimica Acta. 2011;**56**:3884-3889. DOI: 10.1016/j.electacta.2011.02.033

[3] Martín-Palma RJ, McAtee PD, Ramadan R, Lakhtakia A. Hybrid nanostructured porous silicon-silver layers for wideband optical absorption. Scientific Reports. 2019;**9**(1):7291. DOI: 10.1038/s41598-019-43712-7

[4] Irina K, Mihaela M, Mihai D, Monica S, Teodora I, Adina B, et al. Silver/porous silicon (PS) nanocomposite layers for biomedical applications. In: Proceedings of International Semiconductor Conference; 27-29 September; Sinaia. Sinaia: IEEE; 2006. DOI: 10.1109/SMICND.2006.283935

[5] Ensafi AA, Rezaloo F, Rezaei B. Electrochemical sensor based on porous silicon/silver nanocomposite for the determination of hydrogen peroxide. Sensors and Actuators B: Chemical. 2016;**231**:239-244. DOI: 10.1016/j.snb.2016.03.01

[6] Dimitrios PN, Georgia-Paraskevi N, editors. Nanotechnology and Biosensors. 1st ed. United Kingdom: Elsevier; 2018. p. 470. DOI: 10.1016/C2017-0-00358-0

[7] Georgia-Paraskevi N, Dimitrios PN, Christina S, Stephanos K, Spyridoula B, Nikolaos T. Nanobiosensors Based on Graphene Electrodes: Recent Trends and Future Applications. Elsevier; 2018. pp. 161-177. DOI: 10.1016/B978-0-08-101971-9.00007-7. Chapter 6

[8] Zhu Z, Garcia-Gancedo L, Flewitt AJ, Xie H, Moussy F, Milne WI. A critical review of glucose biosensors based on carbon nanomaterials: Carbon nanotubes and graphene. Sensors (Basel). 2012;**12**(5):5996-6022. DOI: 10.3390/s120505996

[9] Ponnusamy R, Chakraborty B, Rout CS. Pd-doped WO_3 nanostructures as potential glucose sensor with insight from electronic structure simulations. The Journal of Physical Chemistry. B. 2018;**122**(10):2737-2746. DOI: 10.1021/acs.jpcb.7b11642

[10] Jiang P, Wang Y, Zhao L, Ji C, Chen D, Nie L. Applications of gold nanoparticles in non-optical biosensors. Nanomaterials (Basel). 2018;**8**(12):977. DOI: 10.3390/nano8120977

[11] Arvind K, Amit S, Ashwani K, Ramesh C. Porous silicon filled with Pd/WO_3–ZnO composite thin film for enhanced H_2 gas-sensing performance. RSC Advances. 2017;**7**:39666-39675. DOI: 10.1039/C7RA05341J

[12] Hamdy ME, Del Carlo M, Hussein HA, Salah TA, El-Deeb AH, Emara MM, et al. Development of gold nanoparticles biosensor for ultrasensitive diagnosis of foot and mouth disease virus. Journal of Nanobiotechnology. 2018;**16**(1):1-12. DOI: 10.1186/s12951-018-0374-x

[13] Zhenga Q, Wua H, Wanga N, Yanc R, Mab Y, Guangb W, et al. Graphene-based biosensors for biomolecules detection. Current Nanoscience. 2014;**10**(5):627-637. DOI: 10.3390/mi11010060

[14] Kim HM, Park JH, Lee SK. Fiber optic sensor based on ZnO nanowires decorated by Au nanoparticles for improved plasmonic biosensor. Scientific Reports. 2019;**9**:15605. DOI: 10.1038/s41598-019-52056-1

[15] Feng C, Xu G, Liu H, Lv J, Zheng Z, Wu Y. Glucose biosensors based on Ag nanoparticles modified TiO_2 nanotube arrays. Journal of Solid State Electrochemistry. 2014;**18**:163-171. DOI: 10.1007/s10008-013-2257-2

[16] Izyumskaya N, Tahira A, Ibupoto ZH, Lewinski N, Avrutin V, Özgür Ü, et al. Electrochemical biosensors based on ZnO nanostructures. ECS Journal of Solid State Science and Technology. 2017;**6**(8):84-100. DOI: 10.1149/2.0291708jss

[17] Szunerits S, Boukherroub R. Graphene-based biosensors. Interface Focus. 2018;**8**:20160132. DOI: 10.1098/rsfs.2016.0132

[18] Bagyalakshmi S, Karthick AA. Study on enzymatic electrochemical glucose biosensors based on ZnO nanorods. International Journal of Scientific Research and Review. 2018;**7**(5):73-81. ISSN: 2279-543X

[19] Said Ragab AM, Hasan MA, Abdelzaher AM, Abdel-Raoof AM. Insights into the developments of nanocomposites for its processing and application as sensing materials. Journal of The Electrochemical Society. 2020;**167**(3):037549. DOI: 10.1149/1945-7111/ab697b

[20] Alabsi SS, Ahmed AY, Dennis JO, Md Khir MH, Algamili AS. A review of carbon nanotubes field effect-based biosensors. IEEE Access. 2020;**8**:69509-69521. DOI: 10.1109/ACCESS.2020.2987204

[21] Nag A, SC Mukhopadhyay SC, Kosel J. Wearable flexible sensors: A review. IEEE Sensors Journal. 2017;**17**(13):3949-3960. DOI: 10.1109/JSEN.2017.2705700

[22] Belorus A, Bespalova K, Spivak Y. Morphology and internal structure of porous silicon powders in dependence on the conditions of post-processing. In: Proceedings of the 2016 IEEE Conference of Russian Young Researchers in Electrical and Electronic Engineering (EIConRus); 2-3 February, 2016; Saint-Petersburg. Moscow: IEEE; 2016. pp. 23-28

[23] Pastukhov A, Belorus A, Bukina Y, Spivak Y, Moshnikov V. Influence of technology conditions on the surface energy of porous silicon using the method of contact angle. In: Proceedings of the 2017 IEEE Conference of Russian Young Researchers in Electrical and Electronic Engineering (EIConRus); 1-3 February, 2017; Saint-Petersburg. Moscow: IEEE; 2017. pp. 1183-1185

[24] Spivak Y, Belorus A, Somov P, Bespalova K, Moshnikov V, Tulenin S. Porous silicon nanoparticles for target drag delivery: Structure and morphology. Journal of Physics Conference Series. 2015;**643**:012022. DOI: 10.1088/1742-6596/643/1/012022

[25] Spivak Y, Belorus A, Moshnikov V, Bespalova K, Somov P, Panevin A, et al. Porous silicon as a nanomaterial for disperse transport systems of targeted drug delivery to the inner ear. The Russian Journal of Applied Physics. 2018;**63**:1352-1360. DOI: 10.1134/S1063784218090207

[26] Permiakov N, Matyushkin L, Belorus A, Koshevoi V. Investigation of a program-controlled process of impregnation of porous semiconductors with silver nanoparticles to create an electrical contact. In: Proceedings of the 2018 IEEE Conference of Russian Young Researchers in Electrical and Electronic Engineering (EIConRus); 29 January–1 February, 2018; Saint-Petersburg. Moscow: IEEE; 2018. pp. 539-543

[27] Belorus A, Pastukhov A, Vasyukov A, Moshnikov V. Formation

of ZnO nanoparticles using electrochemical deposition technique for applications in sensorics and biomedicine. In: 2019 IEEE Conference of Russian Young Researchers in Electrical and Electronic Engineering (EIConRus); 28-31 Jan. 2019; Saint-Petersburg. Moscow: IEEE; 2019. pp. 763-764

[28] Koshevoi V, Belorus A. Study of producing sensors based on porous layers of GaP: Te semiconductors with the use of electrodiffusion contacts. In: Proceedings of the 2017 IEEE Conference of Russian Young Researchers in Electrical and Electronic Engineering (EIConRus); 1-3 February, 2017; Saint-Petersburg. Moscow: IEEE; 2017. pp. 1406-1408

[29] Koshevoi V, Belorus A, Mikhailov I, Tarasov S, Solomonov A, Moshnikov V. Luminescent structures based on porous layers of gallium phosphide including embedded arrays of colloidal quantum dots of cadmium chalcogenides. In: Proceedings of the 2017 IEEE Conference of Russian Young Researchers in Electrical and Electronic Engineering (EIConRus); 1-3 February, 2017; Saint-Petersburg. Moscow: IEEE; 2017. pp. 1457-1459

[30] Pshchelko N, Vodkailo E, Tomaev V, Klimenkov B, Koshevoi V, Belorus A. Influence of electric field on adhesion and structure of conducting films on dielectric substances. Chemistry & Chemical Technology. 2017;**60**:101-104. DOI: 10.6060/tcct.2017608.5649

[31] Zolotarev V. Methods for the Study of Photonics Materials: Elements of Theory and Technology: A Training Manual. St. Petersburg: SPbSU ITMO; 2008. p. 275 (in Russian)

[32] Tolstoy V, Chernyshova I, Skryshevsky V. Handbook of Infrared Spectroscopy of Ultrathin Films. John Wiley & Sons Inc.; 2003. p. 710. DOI: 10.1002/047123432X

[33] Zanoni R, Righini G, Mattogno G, Schirone L, Sotgiu G, Rallod F. X-ray photoelectron spectroscopy characterization of stain-etched luminescent porous silicon films. Journal of Luminescence. 1998;**80**:159-162. DOI: 10.1016/S0022-2313(98)00088-X

[34] Leisenberger F, Duschek R, Czaputa R, Netzer FP, Beamson G, Matthew JAD. A high-resolution XPS study of a complex insulator. Applied Surface Science. 1997;**108**:273-281. DOI: 10.1016/S0169-4332(96)00595-8

[35] Jordan P, Todd G. Simple optical method to determine the porosity of porous silicon films. Thin Solid Films. 2012;**520**:2526-2531. DOI: 10.1016/j.tsf.2011.10.146

[36] Nossarzewska-Orlowska E, Brzozowski A. Photoluminescence properties of porous silicon prepared by electrochemical etching of Si epitaxial layer. In: Proceedings of the XXII International School of Semiconducting Compounds; Jaszowiec. Jaszowiec: Institute of Electronic Materials Technology; 1993. pp. 713-716